EUROPEAN FUSION DEVELOPMENT AGREEMENT

EFDA–JET–PR(03)15

T.C. Hender, D.F. Howell, R.J. Buttery, O. Sauter, F. Sartori, R.J. La Haye,
A.W. Hyatt, C.C. Petty, the DIII-D team and JET EFDA contributors

Comparison of m = 2, n = 1 Neo-classical Tearing Mode Limits in JET and DIII-D

Comparison of m = 2, n = 1 Neo-classical Tearing Mode Limits in JET and DIII-D

T.C. Hender[1], D.F. Howell[1], R.J. Buttery[1], O. Sauter[2], F. Sartori[1]
R J La Haye[3], A W Hyatt[3], C C Petty[3] the DIII-D team
and JET EFDA contributors*

[1]EURATOM/UKAEA Fusion Association, Culham Science Centre, Abingdon, UK
[2]Centre de Recherches en Physique des Plasmas, Association Euratom-Confédération Suisse, EPFL, 1015 Lausanne, Switzerland
[3]General Atomics, San Diego, USA
** See annex of J. Pamela et al, "Overview of Recent JET Results and Future Perspectives", Fusion Energy 2000 (Proc. 18th Int. Conf. Sorrento, 2000), IAEA, Vienna (2001).*

Preprint of Paper to be submitted for publication in
Nuclear Fusion

ABSTRACT.
Joint experiments have been conducted on JET and DIII-D to study m = 2, n = 1 neo-classical tearing modes (NTMs). Very similar instability behaviour is observed on both machines and the scaling of the mode island width with β and the observation of n = 1 islands at q = 2, strongly points to these modes being driven by neo-classical effects. Similarity experiments using closely matched non-dimensional parameters (plasma shape, aspect ratio, q, ρ* and collisionality) on JET and DIII-D show similar global β-limits for the NTM. Further scalings, which combine broader data sets from JET and DIII-D, show an approximately linear scaling, or slightly stronger, with ion gyro-radius and a relatively weak dependence on collisionality.

1. INTRODUCTION

Previous studies [e.g. 1,2,3,4] have largely focused on the stability of the (3,2) neo-classical tearing modes (NTMs) (where the (m,n) notation describes the poloidal and toroidal mode numbers, respectively). This mode is generally found to limit performance by causing a moderate degradation in energy confinement (~10 to 20%) and is found to have a threshold in normalised β, $\beta_N = 2\mu_0 \langle p \rangle / B_t^2 / (I(MA)/a(m)B_t(T))$ [with $\langle\ \rangle$ denoting a volume average, B_t the vacuum toroidal field, a the plasma minor radius, and I the plasma current], which scales approximately linearly with the normalised ion gyro-radius (defined here for a pure deuterium plasma)

$$\rho^*_{tor} = \frac{2.04 \times 10^{-4} \sqrt{T_i(eV)}}{aB_t} \qquad (1)$$

for the present range of experimental parameters. While less studied, the (2,1) NTM is potentially more serious as it always leads to severe energy confinement degradation and can lead to disruptions (or a termination of the discharge by the machine protection systems). It is therefore important to determine the scaling behaviour for the (2,1) NTM. In such determinations, cross machine data sets are especially valuable since they extend the range of non-dimensional parameters and by virtue of the extended range of dimensional parameters (size, magnetic field etc) provide a more stringent test of the physics models. To this end detailed scans of the (2,1) NTM β-limits have been performed on the JET and DIII-D tokamaks. Some of the DIII-D pulses are matched in plasma shape and normalised current $[I_N = I(MA)/a(m)B_t(T)]$ to corresponding JET pulses; this allows direct comparison of the (2,1) β_N-limits in global non-dimensional parameters between JET and DIII-D. Further, by making comparisons in local non-dimensional parameters, data-sets with different plasma shapes and I_N values can be mixed, and scalings in the non-dimensional parameters determined.

In the next section details of the experimental method are given, with the scaling results being presented in Section 3 and conclusions given in Section 4.

2. EXPERIMENT DETAILS

On JET the plasmas used in the (2,1) NTM experiments were a standard low triangularity (δ=0.23)

configuration with an elongation κ=1.7 and an aspect ratio, $R_0/a \approx 3.3$. On DIII-D two plasma shapes were used, one of which was designed to closely mimic the JET shape and a more standard DIII-D shape which has a somewhat lower aspect ratio, $R_0/a \approx 2.8$; the plasma shapes used are summarised in Fig1.

The experiments described here use neutral beam injection (NBI) heating solely to raise the plasma pressure and destabilise the NTM; though there are observations on JET of (2,1) NTMs destabilised using ion cyclotron heating. With the available NBI heating, JET discharges with q_{95}~3 to 3.5 are limited to a toroidal field, $B_t \lesssim 1.1$T, if (2,1) NTMs are to be destabilised. Part of the aim of the experiments described here is to compare (2,1) β-limits in JET and DIII-D at the same global non-dimensional parameters. Defining an average density n_a to be the line average value and an average temperature $T_a = \langle p \rangle / (k n_a)$ then the global normalised gyro-radius (Eqn 1 using T_a) being constant implies $T_a \sim a^2 B^2$ and global normalised collisionality (defined with respect to the gyro-bounce time, ν^* [cf Eq 2]) being constant implies $n_a \sim a^3 B^4$. If β is constant (which is not a priori guaranteed as the (2,1) β-limit might be different in JET and DIII-D at the same ρ^* and ν^*) then $a^{1.25}B$ will be constant. For the minimum field (0.95T) and average electron density (2.6×10^{19} m^{-3}) at which NTMs have been studied on JET, this implies the same non-dimensional parameters (ρ^*, ν^*, β) would be achieved in DIII-D at 1.9T and 7.6×10^{19} m^{-3}, which as described below is closely, but not exactly, achievable because of NBI power limitations.

Experimentally the procedure used on JET and DIII-D is very similar. A target L-mode sawtoothing discharge is established and then the NBI power is gradually ramped (with a consequent transition to ELMy H-mode) to determine the (2,1) NTM b-limit. In nearly all cases, on both machines, a (3,2) mode is destabilised at lower b and so precedes the (2,1) mode. Once destabilised the (2,1) mode grows rapidly and becomes sufficiently large to cause the mode to lock or rotate very slowly. The effect of the large (2,1) is to cause a substantial energy loss which may stabilise the mode, or the discharge may disrupt before that occurs. Figure 2 shows the time histories of typical discharges on JET and DIII-D, and Fig.3 compares a spectrogram of an outboard Mirnov probe for typical discharges on JET and DIII-D; the close similarity of behaviour on the 2 machines is evident.

One issue to address is the neo-classical nature of these modes. Figure 4 shows the square root of the odd-n radial field amplitude as a function of β_N for several JET and DIII-D discharges. For NTMs the island width ($\propto\sqrt{}$[radial field]) should scale with β provided the mode is sufficiently large so as not to be significantly affected by the finite island width threshold terms (such as that from the polarisation current model [5]). From Fig 4 it can be seen that the island width does indeed scale approximately linearly with b. Another characteristic of NTMs is of course the existence of magnetic islands. Figure 5 shows contours of electron temperature (measured by electron cyclotron emission) in DIII-D at the time just before mode locking occurs due to the (2,1) mode. Clear n=1 islands can be seen at q=2 in Fig.5 and a distorted n=2 island chain can be seen at q=1.5. The final typical characteristic of NTMs is that they are metastable and require a seed perturbation to initiate their growth. This characteristic is also often manifested by a hysteresis, with the mode disappearing at a lower β_N than that at which it is formed by the seed perturbation. In DIII-D the initiation of the (2,1) mode can be attributed to an

ELM in some cases. In JET the seeding of the (2,1) mode is less clear except at low-q_{95} (<3) where combined sawteeth-ELMs clearly act as seeds, though the related characteristic of a significant hysteresis in bN is evident in JET. It is possible in both machines that the (2,1) mode growth starts as a classical tearing mode in some cases, as the bN can be close to the ideal limit [6]. So, although it is not possible to be certain, the (2,1) modes in JET and DIII-D certainly have the main characteristics of NTMs.

3. SCALINGS

The dimensionless scalings discussed in the previous section show that if the (2,1) b–limit is the same in DIII-D and JET, then at the same ρ^*, ν^* one should scale the toroidal field with $Ba^{1.25}$ constant, and scale the density as a^3B^4. Here the standard definition of ν^*, normalised to bounce frequency is assumed. In NTM studies an alternate normalisation, suggested by the polarisation theory model [5], of ν^* normalised with respect to the diamagnetic frequency [4] is often used. In fact since these two definitions of ν^* differ by a factor proportional to ρ^*, it does not matter which ν^* definition is used in comparing dimensionally similar discharges.

Since NTMs are driven by local gradients, for global scaling comparisons to be valid, the plasma profiles will need to be equivalent in JET and DIII-D. Figure 6 shows that the scaled profiles between JET and DIII-D do indeed have very similar shapes. Figure 7 shows the data set of JET-shape DIII-D (2,1) NTM bN-limits are compared with a few JET pulses scaled using the non-dimensional scalings; it can be seen that although the data sets do not quite overlap, the JET bN values are consistent with the DIII-D results; parameters for several dimensionally similar shots, from JET and DIII-D, are summarised in Table I. These results seem to indicate, in a similar fashion to confinement similarity experiments [7], that (2,1) NTM b-limits obey dimensional scalings; for completeness confinement scalings are also compared in Table I though it should be noted at the times compared confinement is being affected by the presence of a (3,2) NTM. An issue here is that the bN values compared are from diamagnetic measurements and therefore include fast particle contributions which are rather higher in the lower density JET discharges. It is not totally clear how the fast particle element should be treated in terms of its ability to drive bootstrap current but to examine consistency of thermal bN limits it is necessary to also scale between cases using thermally derived ρ^* and ν^* values; such a comparison is made below (cf Fig 8a) and found to be favourable.

Three comparisons of the data have been made in local dimensionless parameters. The collisionality normalised to the bounce frequency is defined as

$$\nu^* = \frac{520 n_e (10^{19} m^{-3}) R q}{\varepsilon^{3/2} T_i^2 (eV)} \qquad (2)$$

a local poloidal β is defined as

$$\nu_{pe} = \frac{2\mu_0 P_e}{B_\vartheta{}^2} \qquad (3)$$

and the normalised poloidal gyro-radius is

$$\rho_\theta^* = \frac{2.04\times10^{-4}\sqrt{T_i(eV)}}{r_s B_\theta} \quad (4)$$

where all quantities are at the outboard mid-plane, P_e is the electron pressure, B_θ the q=2 surface flux surface averaged poloidal field, r_s is the q=2 radius and a the minor radius; with all units SI unless otherwise stated. The local drive for the NTM is given proportional to $L_q\,\beta_{pe}\,J_{boot}$, where L_q=q/q' (with q' being the derivative with respect to minor radius) and the bootstrap current (J_{boot}) is evaluated using expressions given in Ref [9] (with the trapped particle fraction approximated as an aspect ratio expansion). Since local parameters are being used, data from both DIII-D plasma shapes (see Fig.1) can be included in these scaling studies. The scaling of thermal β_N is found to be

$$\beta_N\,(\text{thermal}) = 550\,(\rho^*)^{1.02\pm0.16}\;\nu^{*0.19\pm0.03} \quad (5)$$

the scaling of the local β_p is found to be

$$\beta_{pe} = 101\,(\rho_\theta^*)^{1.59\pm0.12}\,(\nu^*)^{0.37\pm0.05} \quad (6)$$

and the fit with the bootstrap drive term is

$$L_q\,\beta_{pe}\,J_{boot} = 36.4\,(\rho_\theta^*)^{1.28\pm0.1}\,(\nu^*)^{0.21\pm0.03} \quad (7)$$

The coefficient of determination for the local β_p fit is R^2 = 0.79, while for the thermal β_N fit it is R^2 = 0.57 and for the bootstrap drive term is R^2 =0.74. The quality of the β_N, bp and bootstrap drive ($L_q\,\beta_{pe}\,J_{boot}$) fits are summarised in Fig.8. For the β_N fit the quality is improved by fitting in thermal rather than total bN because of the rather different fast particle fractions; the lower densities in JET mean the fast particle fraction (34% average) is higher than DIII-D with the JET shape (24% average) or with its standard shape (16% average). For the local β_p fits (Eqs 6 and 7) it can be seen from Fig.8 that the JET and JET-shape DIII-D data seem to have a slightly different slope than the equality fit line; it should be noted that this discrepancy is not resolved by excluding the standard shape DIII-D data from the fit and may indicate a hidden variable playing a role in determining the β-limit.

4. SUMMARY

Joint experiments have been conducted on JET and DIII-D to study (2,1) NTMs. Very similar instability behaviour is observed on both machines, with the (2,1) mode growing rapidly and locking; this always leads to a severe energy degradation and sometimes to a disruption. The scaling of the (2,1) mode island width with β and the observation of (2,1) islands in ECE temperature data, strongly point to these modes being dominantly driven by neo-classical effects. Similarity experiments using closely

matched non-dimensional parameters (aspect ratio, shape, q, ρ^* and collisionality) on JET and DIII-D show similar β-limits for the (2,1) NTM. Further scalings, which combine broader data sets from JET and DIII-D, show a linear, or slightly stronger, scaling with ρ^* and a relatively weak dependence on collisionality - a result which is very similar to scalings observed for the (3,2) NTM.

ACKNOWLEDGEMENTS

This work was partly performed under the European Fusion Development Agreement. The authors were in part funded by the United Kingdom Engineering and Physical Sciences Research Council and by EURATOM, in part by the Swiss National Science Foundation and in part by the US DoE under grant No DE-AC03-99ER55463.

REFERENCES

[1]. CHANG, Z., et al., "Observation of neoclassical pressure-gradient-driven tearing mode in TFTR", Phys Rev Lett **74** (1995) 4663.

[2]. HUYSMANS, G.T.A., "Observation of neoclassical tearing modes in JET", Fusion Energy 1998 (Proc. 17th Int. Conf. Yokahama, 1998) IAEA Vienna (1999) (CD-R file EXP3/103)

[3]. GUENTER, S., "Influence of neoclassical tearing modes on energy confinement" et al., Plasma Phys and Contr Fus **41** (1999) 767.

[4]. LA HAYE, R.J., et al, "Dimensionless scaling of the critical beta for onset of a neo-classical tearing mode", Phys of Plasmas **7** (2000) 3349.

[5]. WILSON, H.R., et al., "Threshold for neoclassical magnetic islands in a low collision frequency tokamak", Phys Plasmas **3** (1996) 248.

[6]. Brennan, D P, et al, "Tearing Mode Stability Studies Near Ideal Stability Boundaries in DIII-D", Phys. Plasmas **9**, (2002) 2998.

[7]. PETTY, C. C. et al., Phys. Plasmas **5** (1998) 1695.

[8]. CHRISTIANSEN, J et al. Nucl Fusion **38** (1998) 1757.

[9]. SAUTER, O et al, Phys of Plasmas **6** (1999) 2834.

Pulse No:	**53223**	**53225**	**106781**	**107758**
Machine	JET	JET	DIII-D	DIII-D
I_p (MA)	0.95	0.96	0.94	1.06
B_t (T)	0.97	0.97	1.70	1.89
$B_t a^{5/4}$ ($Tm^{5/4}$)	0.83	0.84	0.79	0.87
n_e (10^{19} m^{-3})	2.55	2.60	6.95	6.6
$n_e a^2$ (10^{19} m^{-1})	2.00	2.05	2.03	1.92
Global ρ^*	2.6×10^{-4}	2.5×10^{-4}	2.7×10^{-4}	2.7×10^{-4}
Global ν^*	2.2×10^{-3}	2.8×10^{-3}	3.1×10^{-3}	1.9×10^{-3}
β_n (%mTMA^{-1})	3.8	3.6	3.8	3.7
$B_t \beta_{th}$ (Ts)	0.081	0.124	0.104	0.118
$\omega_{q=2}$ (10^4 s^{-1})	1.3	1.5	2.6	3.2

Table I Comparison of dimensionally similar discharges in JET and DIII-D, where parameter values are at the time the m=2, n=1 mode is destabilised. The global ρ^* and ν^* are defined in Ref [8]. In dimensionally matched discharges then the normalised thermal confinement time ($B_t\tau_{th}$) should agree (though it should be noted these discharges are not in steady state, i.e. dW/dt≠0). Finally angular frequency (ω_q=2) measured by charge exchange at q=2 is shown.

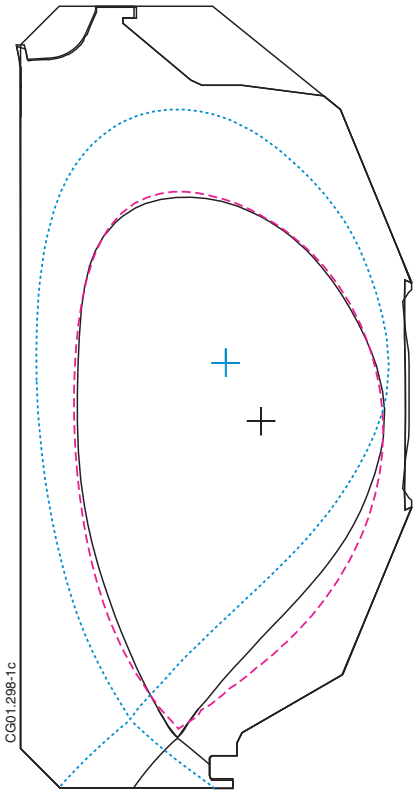

Figure 1: Comparison of plasma boundary shapes used in the (2,1) NTM experiments. The standard DIII-D shape is shown by the short broken line, while the JET-shape DIII-D plasma shown by the solid line is compared with the JET boundary shape (scaled by 59% from R=2.96m) shown by the long broken line.

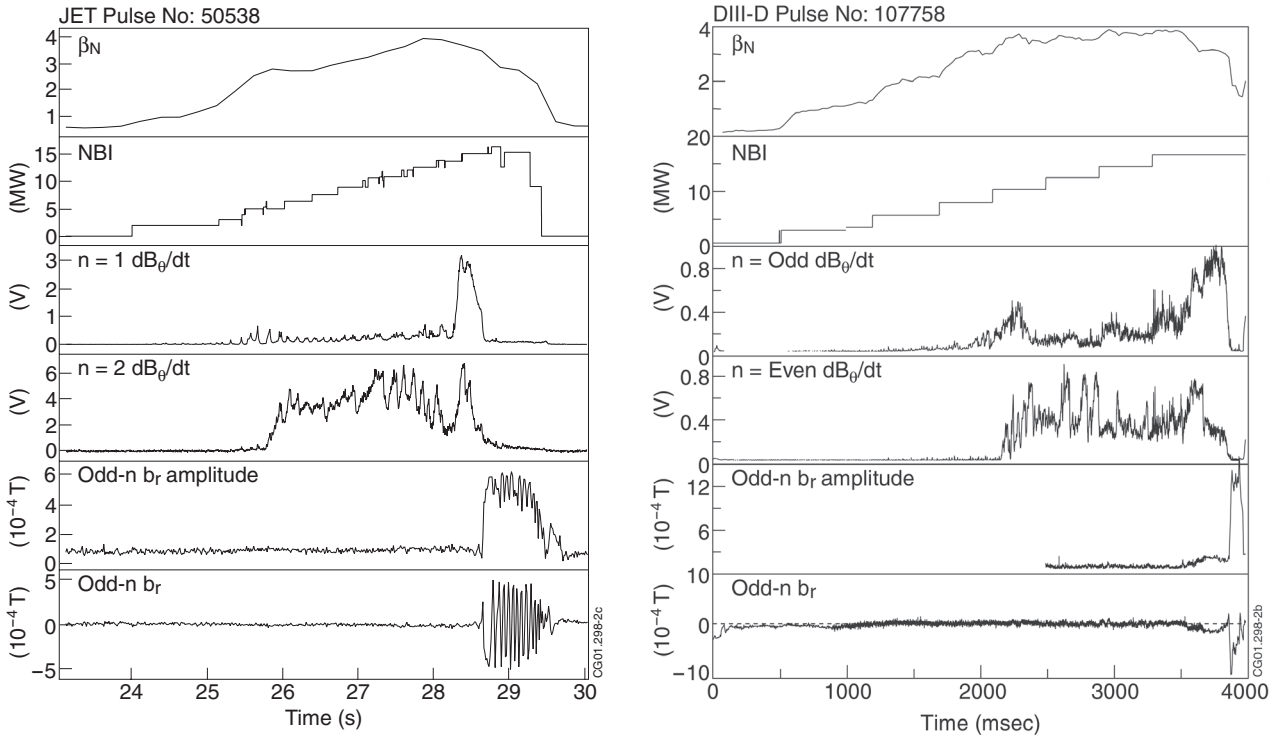

Figure 2: (a) Typical JET pulse (I_p=0.95MA, B_t=0.97T) in which the β_N-threshold for the (2,1) NTM is determined. The NBI power is ramped slowly causing a (3,2) NTM to be destabilised at 25.7s with a noticeable confinement degradation. At higher NBI power, and bN, the (2,1) NTM destabilised. This mode grows rapidly and becomes slowly rotating with a large confinement degradation. (b) Typical DIII-D pulse (I_p=1.06MA, B_t=1.91T) showing very similar behaviour with a (3,2) mode forming at 2150ms and the (2,1) mode starting at 3500ms.

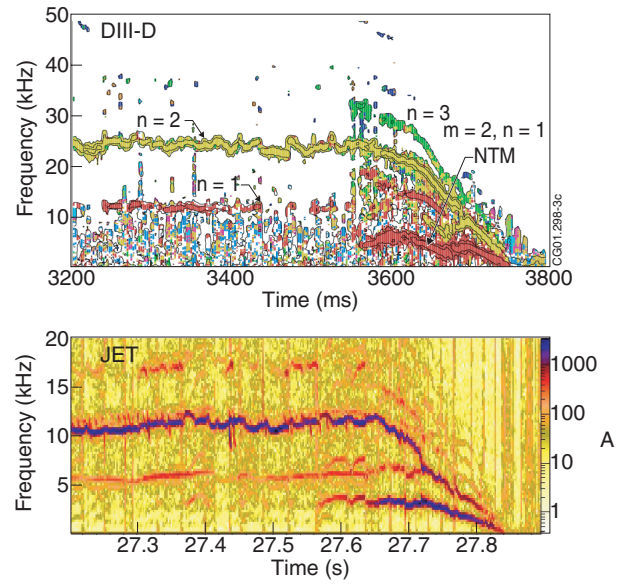

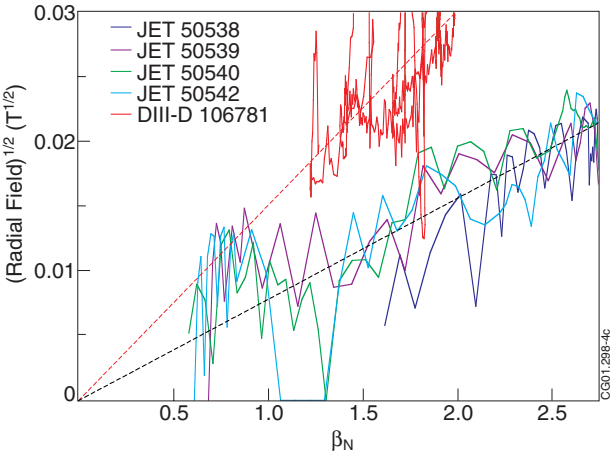

Figure 3: (a) Showing development of the (2,1) NTM in DIII-D pulse 106863. The (3,2) NTM starts considerably earlier at 1450ms. (b) The very similar behaviour in JET pulse 50694 where the (3,2) NTM starts 25.56s.

Figure 4: Radial field amplitude as function of β_N, when there is a locked or a slowly rotating mode. A set of 4 consecutive JET pulses which form NTMs are shown and a pulse from DIII-D is shown too.

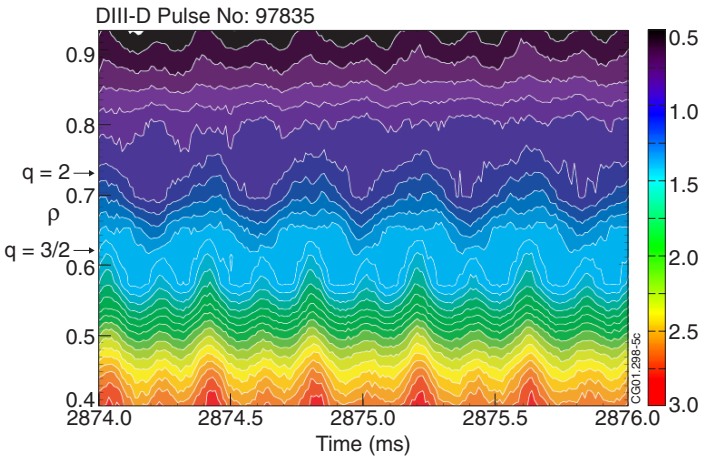

Figure 5: Electron temperature (in keV) contours for DIII-D pulse 97835 (ρ is the square root of toroidal flux). The q values determined from EFIT are marked. Note the q=2 islands and the strongly distorted n=2 islands at q=3/2.

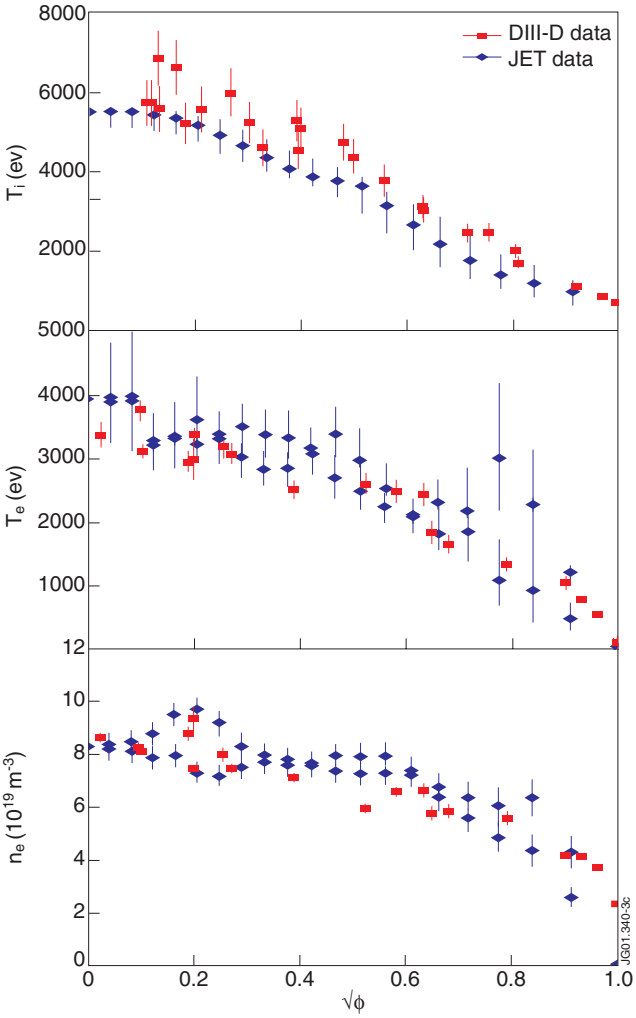

Figure 6: Comparison of ion temperature profiles, electron temperature profiles and density profiles (53223) and a JET-shape DIII-D case (107758). The radial variable used is the square root of normalised toroidal flux. The JET data are scaled to DIII-D size according to non-dimensional scalings (na^2 and $Ta^{0.5}$ constant). The density for the DIII-D case is slightly below that required for a non-dimensional match and correspondingly the temperature is slightly above.

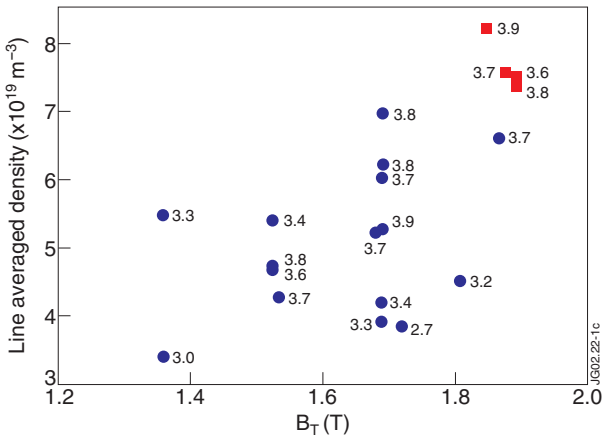

Figure 7: JET-shape DIII-D data for the onset of the (2,1) NTM (circles) and some JET cases scaled at constant ρ, ν* and β_N to DIII-D dimensions (squares). The β_N is indicated for each case.*

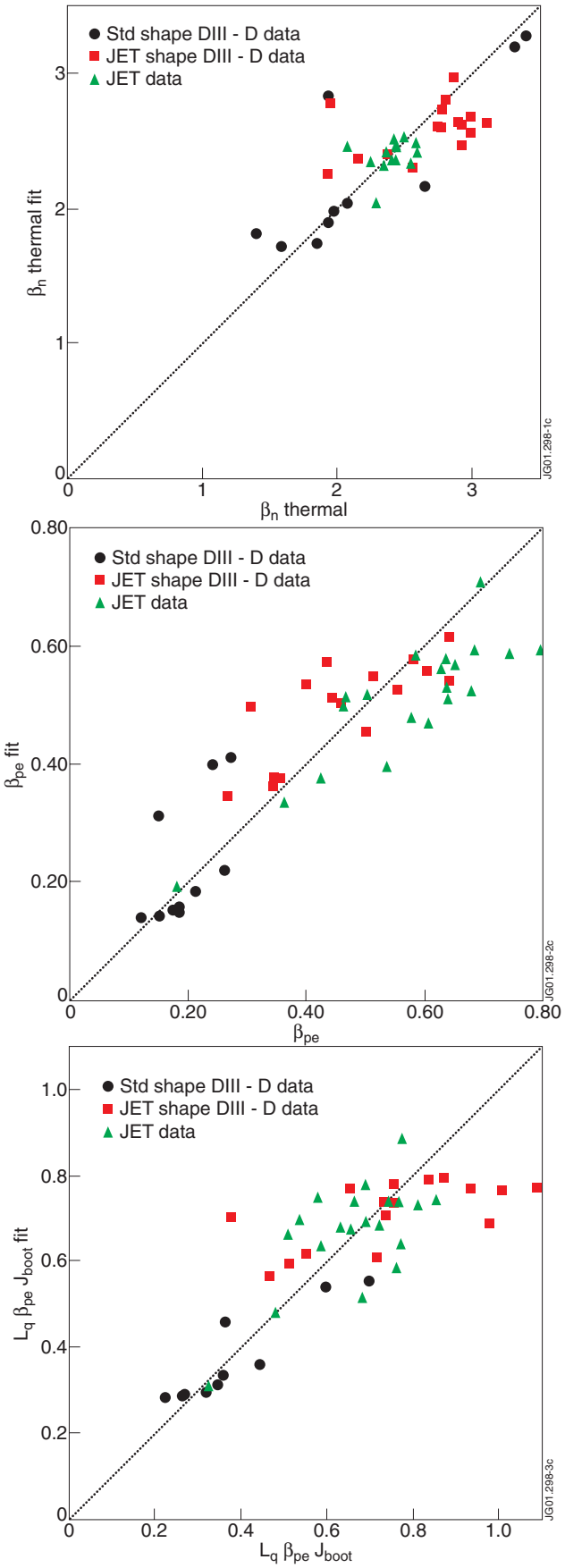

Figure 8: Comparisons of thermal β_N fit ($\propto(\rho^*)^{1.02}\,(\nu^*)^{0.19}$), local bp fit ($\propto(\rho_\theta^*)^{1.59}\,(\nu^*)^{0.37}$) and local bootstrap drive fit ($\propto(\rho_\theta^*)^{1.28}\,(\nu^*)^{0.21}$) [Eqns 5, 6 and 7] for the (2,1) NTM threshold with actual values. For the β_N thermal fit the JET data range is restricted to $3.2<q_{95}<3.8$, but the full range $2.4<q_{95}<4.1$ is included in the 2 local β_p fits.